Comptes Rendus
Chimie
Supplementary material to the article available at:
https://doi.org/10.5802/crchim.172

Supplementary material: Liquid–liquid extraction: thermodynamics–kinetics driven processes explored by microfluidics

Document complémentaire : Extraction liquide–liquide : processus sous contrôle thermodynamique–cinétique explorés par la microfluidique

Fabien Olivier[a, b], **Ange A. Maurice**[b], **Daniel Meyer**[c] **and Jean-Christophe P. Gabriel**[*, a, b]

[a] Université Paris-Saclay, CEA, CNRS, NIMBE, LICSEN, F-91191, Gif-Sur-Yvette, France

[b] SCARCE Laboratory, Energy Research Institute @ NTU (ERI@N), Nanyang Technological University, 637553, Singapore

[c] Institut de Chimie Séparative de Marcoule (ICSM), Université de Montpellier, CEA, CNRS, ENSCM, UMR 5257, Bâtiment 426, BP 17171, 30207 Bagnols-sur-Cèze, France

E-mails: FABIENLO001@e.ntu.edu.sg (F. Olivier), amaurice@pa.uc3m.es (A. A. Maurice), daniel.meyer@cea.fr (D. Meyer), jean-christophe.gabriel@cea.fr (J.-C. P. Gabriel)

[*] Corresponding author.

1. XRF calibration

Multiple known concentrations of Yb^{3+} and Fe^{3+} in the organic medium and aqueous medium were prepared by dilution of standard solutions of known concentration for both Yb^{3+} and Fe^{3+} in organic and aqueous, respectively. The concentrations of all two elements (Yb^{3+} and Fe^{3+}) in the aqueous and organic medium were generated randomly and uniformly within a given range (Table S1). According to the procedure described in references [1,2]; standard known concentrations solutions of single element and mixture of the two were prepared.

Figure shows the calibration curves obtained from measuring the solutions listed in Table S1. The following energy ranges were integrated for Fe: 6.08–6.82 keV and Yb: 7.13–7.88 keV.

To assess the accuracy of the calibration, the results were cross-validated using the scikit-learn library in Python. Measurement error likely arises from matrix effects, which induce unwanted correlation between element peaks.

Supplementary Table S1. Calibration concentrations of Fe^{3+} and Yb^{3+} in organic and aqueous phases

Organic samples	Fe^{3+} (mM)	Yb^{3+} (mM)	Aqueous samples	Fe^{3+} (mM)	Yb^{3+} (mM)
1	4	9	16	10	5
2	5	5	17	7	6
3	3	4	18	4	9
4	2	8	19	2	8
5	1	9	20	5	5
6	10	5	21	1	9
7	6	8	22	9	2
8	7	6	23	3	4
9	9	2	24	6	8
10	12	0	25	12	0
11	6	0	26	6	0
12	1	0	27	1	0
13	0	1	28	0	1
14	0	6	29	0	6
15	0	12	30	0	12

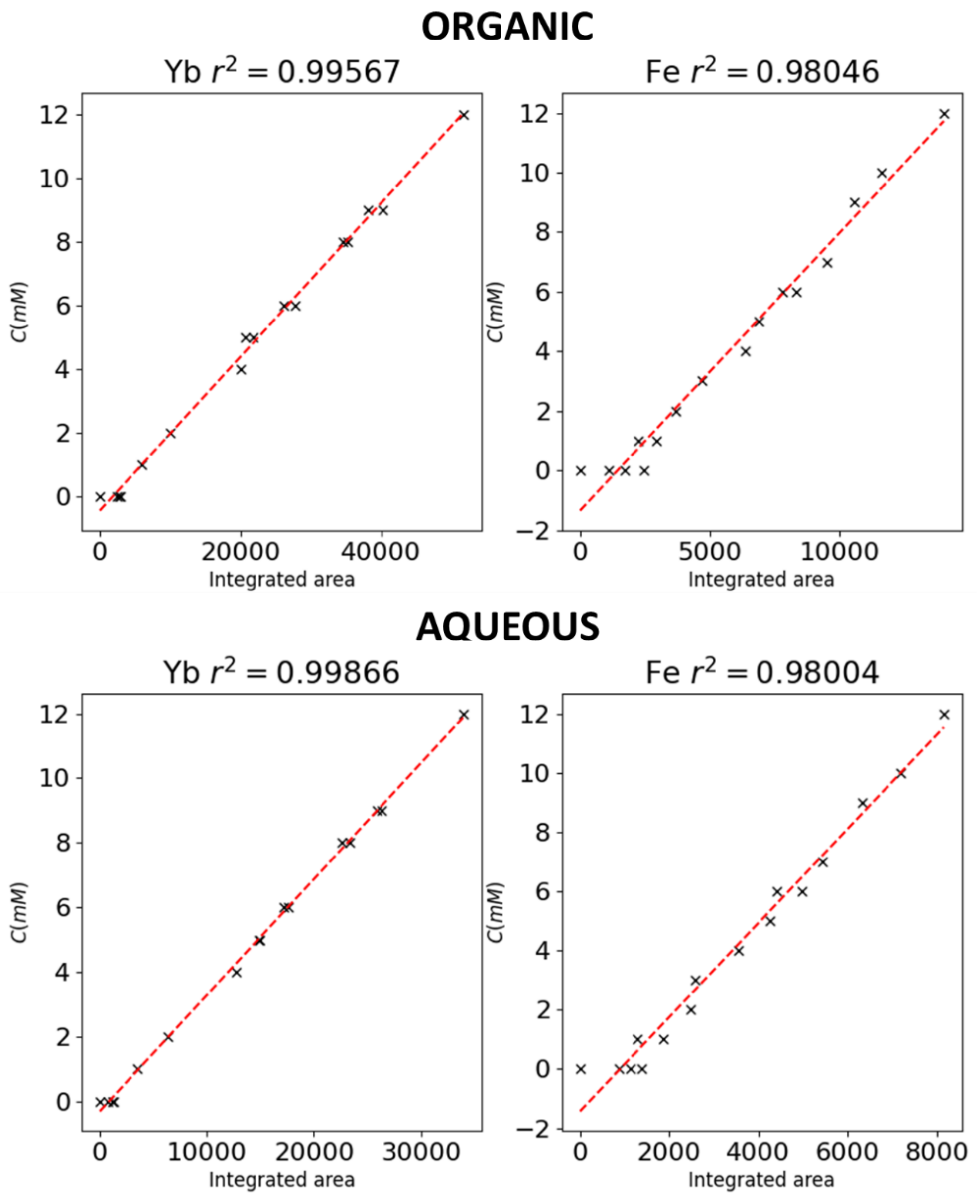

Supplementary Figure S2. Calibration curves of the XRF chip.

2. Kinetics data

Microfluidics output metal concentration as a function of time for liquid–liquid extractions and reverse extractions at 20, 30 and 35 °C are presented in Figure S3. These raw data show particularly the different kinetic behaviour of Yb^{3+} and Fe^{3+}. Also, negative spikes are observed in rare occasion, which are the signature of a microbubble of air passing in the microfluidic channel.

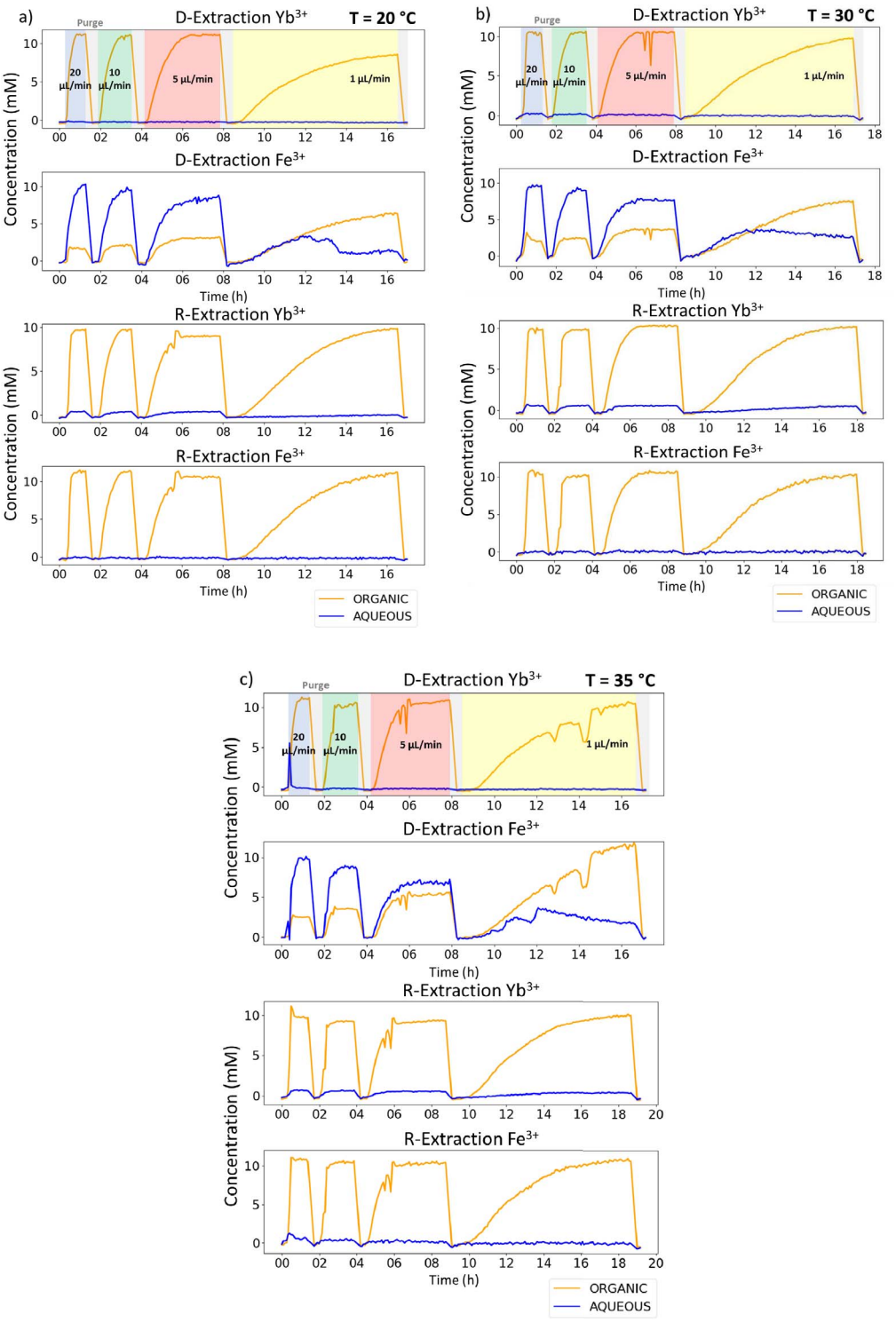

Supplementary Figure S3. Kinetic data for liquid–liquid extractions and reverse extractions at (a) 25 °C, (b) 30 °C and (c) 35 °C.

Supplementary Table S2. Extraction ratios for each contact time and temperature for direct extraction of Fe^{3+} and Yb^{3+}

Contact time (min)	Temperature (°C)	D-extraction Fe^{3+} $\frac{[Fe^{3+}]_{org}^{Out}}{[Fe^{3+}]_{aq}^{In}}$	D-extraction Yb^{3+} $\frac{[Yb^{3+}]_{org}^{Out}}{[Yb^{3+}]_{aq}^{In}}$
1.7	20 °C	9.09 ± 7.57	95.45 ± 0.21
	25 °C	4.55 ± 14.22	90.91 ± 0.20
	30 °C	13.64 ± 4.31	95.45 ± 0.11
	35 °C	13.64 ± 4.34	95.45 ± 0.18
3.4	20 °C	13.64 ± 5.05	95.45 ± 0.14
	25 °C	9.09 ± 7.02	95.45 ± 0.11
	30 °C	13.64 ± 4.13	95.45 ± 0.10
	35 °C	22.73 ± 2.61	95.45 ± 0.14
6.8	20 °C	22.73 ± 3.03	95.45 ± 0.13
	25 °C	22.73 ± 2.83	95.45 ± 0.11
	30 °C	27.27 ± 2.07	95.45 ± 0.10
	35 °C	40.91 ± 1.46	95.45 ± 0.12
34	20 °C	59.09 ± 1.16	81.82 ± 0.15
	25 °C	63.64 ± 1.02	81.82 ± 0.13
	30 °C	72.73 ± 0.78	90.91 ± 0.11
	35 °C	95.45 ± 0.64	95.45 ± 0.13

3. Extraction ratios

Table S2 gives all the extraction ratios obtained for Yb^{3+} and Fe^{3+} for each direct extraction. Table S3 summarises the amount (in %) for each species which is remaining at steady state on the organic side. Hence, ratios obtained in D-extraction and R-extraction can be compared.

4. Distribution ratios for ΔG calculation

For a liquid–liquid extraction system where a species X is extracted, its corresponding distribution ratio can be calculated as follows:

$$K_d(X) = \frac{[X]_{org}^{eq}}{[X]_{aq}^{eq}} \tag{S1}$$

where $[X]_{org}^{eq}$ and $[X]_{aq}^{eq}$ are the concentrations taken at thermodynamic equilibrium respectively in from the organic and the aqueous phases.

One can note that K_d is involved in the calculation of G (see (S2)) as follows:

$$\Delta G(M) = -RT\ln(K_d(M)) \tag{S2}$$

Table S4 summarises the distribution ratios for reverse extraction of Yb^{3+} and Fe^{3+}.

Supplementary Table S3. Percentage of Fe^{3+} and Yb^{3+} remaining in the organic phase at steady state for each contact time and temperature for reverse extraction

Contact time (min)	Temperature (°C)	R-extraction Fe^{3+} $\frac{[Fe^{3+}]_{org}^{Out}}{[Fe^{3+}]_{org}^{In}}$	R-extraction Yb^{3+} $\frac{[Yb^{3+}]_{org}^{Out}}{[Yb^{3+}]_{org}^{In}}$
1.7	20 °C	95.45 ± 0.56	86.36 ± 0.12
	25 °C	95.45 ± 0.57	86.36 ± 0.12
	30 °C	95.45 ± 0.55	81.82 ± 0.12
	35 °C	95.45 ± 0.56	90.91 ± 0.11
3.4	20 °C	95.00 ± 1.14	90.91 ± 0.32
	25 °C	95.00 ± 0.72	90.91 ± 0.13
	30 °C	95.00 ± 0.72	90.91 ± 0.12
	35 °C	95.00 ± 0.72	90.91 ± 0.12
6.8	20 °C	81.82 ± 0.80	90.91 ± 0.15
	25 °C	77.27 ± 0.82	90.91 ± 0.13
	30 °C	77.27 ± 0.82	95.45 ± 0.13
	35 °C	77.27 ± 0.82	90.91 ± 0.13
34	20 °C	72.73 ± 0.98	90.91 ± 0.13
	25 °C	72.73 ± 0.99	86.36 ± 0.13
	30 °C	72.73 ± 0.98	86.36 ± 0.13
	35 °C	72.73 ± 0.99	90.91 ± 0.13

Supplementary Table S4. Distribution ratios for reverse extractions of Yb^{3+} and Fe^{3+} for each temperature

Temperature (°C)	R-extraction Fe^{3+}	R-extraction Yb^{3+}
20	21 ± 51	6.8 ± 4.5
25	19 ± 44	10 ± 8
30	3.7 ± 2.1	13 ± 14
35	2.7 ± 1.1	8.2 ± 6.0

References

[1] D. Kirsanov, V. Panchuk, M. Agafonova-Moroz, M. Khaydukova, A. Lumpov, V. Semenov, A. Legin, *Analyst*, 2014, **139**, 4303-4309.

[2] A. El Maangar, J. Theisen, C. Penisson, T. Zemb, J.-C. P. Gabriel, *Phys. Chem. Chem. Phys.*, 2020, **22**, 5449-5462.